Ecological Modelling, 33 (1986) 231–253
Elsevier Science Publishers B.V., Amsterdam – Printed in The Netherlands

ACIDIFICATION OF FOREST SOILS: MODEL DEVELOPMENT AND APPLICATION FOR ANALYZING IMPACTS OF ACIDIC DEPOSITION IN EUROPE

PEKKA KAUPPI, JUHA KÄMÄRI, MAXIMILIAN POSCH, LEA KAUPPI
International Institute for Applied Systems Analysis, A-2361 Laxenburg (Austria)

and EGBERT MATZNER

Research Center for Forest Ecosystem / Forest Decline, University of Göttingen, Büsgenweg 2, D-3400 Göttingen, (Federal Republic of Germany)

(Accepted 17 July 1985)

ABSTRACT

Kauppi, P., Kämäri, J., Posch, M., Kauppi, L. and Matzner, E., 1986. Acidification of forest soils: model development and application for analyzing impacts of acidic deposition in Europe. *Ecol. Modelling*, 33: 231–253.

Acidification is considered to be an unfavourable process in forest soil. Timber logging, natural accumulation of biomass in the ecosystem, and acidic deposition are known sources of acidification. Acidification causes a risk of damage to plant roots and subsequent risk of a decline in ecosystem productivity.

A dynamic model is introduced for describing the acidification of forest soils. In 1-year time steps the model calculates the soil pH as a function of the acid stress and the buffer mechanisms of the soil. Acid stress is defined as the hydrogen ion input into the top soil. The buffer mechanisms counteract acidification by providing a sink for hydrogen ions. The concepts *buffer rate* and *buffer capacity* are used to quantify the buffer mechanisms. The model compares (a) the rate of acid stress (annual amount) with the buffer rate, and (b) the accumulated acid stress (over several years) with the buffer capacity. These two comparisons give an estimate of the soil acidity.

The model was incorporated into the Regional Acidification INformation and Simulation (RAINS) model system of the International Institute for Applied Systems Analysis for analyzing the acidic deposition problem in Europe. This system links information on energy production, pollutant emission, pollutant transport, and pollutant deposition. The data on acid stress entering the soils was obtained from other submodels. Data on buffer rate and buffer capacity were collected from soil maps and geological maps.

The model system as a whole is now available for analyzing the impact of different emission scenarios. The soil acidification model assumes sulfur deposition estimates from the other submodels as input, and as output it produces estimates of the acidity of European forest soils in a map format. Additionally it computes the total area of forests in Europe with the estimated soil pH lower than any selected threshold value. Sources of uncertainty in the soil acidification model are listed and briefly evaluated.

0304-3800/86/$03.50

INTRODUCTION

Extensive forest damage has been observed in rural areas of Central Europe since the 1970's. It was first reported on silver fir (Schütt, 1977) and later on Norway spruce, Scots pine, beech, and other tree species (Schütt et al., 1983). In 1984, in the Federal Republic of Germany damage was reported for a forest area of 2 549 000 ha (Lammel, 1984). Forest damage is a result of many factors including the direct impact of air pollutants on tree foliage, soil acidification, and climate. In this study we concentrate on soil acidification, which has been demonstrated as an important link between air pollution and forest damage. It is intended that other factors contributing to the forest damage will be incorporated into the model as soon as possible.

The study includes model development and model application. The main objective of the study is to develop a method for computing the time evolution of acidification of forest soils. An additional objective is to apply the model for getting an overview of the forest soil acidification due to air pollution at the European level.

SOIL ACIDIFICATION

Soil acidification has been defined as being a decrease in the acid neutralization capacity of the soil (Van Breemen et al., 1984). Such a decrease may coincide with a decrease in soil pH. It may also take place in conditions of a relatively constant pH assuming efficient buffering processes. In such a case the buffering of the soil counteracts the effect of acidic deposition or biomass removal, so that over long periods of time the soil pH remains stable. Nevertheless the neutralization capacity is being depleted and the soil is subject to acidification.

Acid stress

Acid stress is defined as the input of hydrogen ions into the top-soil. Acid stress can result from acidic deposition of air pollutants, from biomass utilization, and from the natural biological activity of ecosystems (Ulrich, 1983a; Van Breemen et al., 1984). Any one of these sources can dominate the stream of protons entering the soil. The acid stress due to air pollution can result from the direct deposition of hydrogen ions or from the indirect effect of acid-producing substances such as the dry deposition of SO_2.

Acid stress has two important aspects. One is the accumulative load of the stress and the other is the instantaneous rate of the stress. The variable *amount of stress* refers to the load, and involves accumulation over several

years. The unit for the amount of stress is kilomoles of acidity per hectare (kmol ha^{-1}). The variable *stress rate* refers, in principle, to the time derivative of the amount of stress although in practice it is given as annual hydrogen ion input. The unit for the stress rate is kilomoles of acidity per hectare per year (kmol ha^{-1} $year^{-1}$).

Buffering processes

Soil reacts to acid stress depending on the soil properties. Acid stress implies influx of hydrogen ions, and in the corresponding way the buffering properties of the soil imply consumption of hydrogen ions. Buffering is described using two variables, one for the gross potential and the other for the rate of the reaction. Both variables refer to the intrinsic properties of the soil and can be quantified after fixing the volume of the reacting soil layer.

Buffer capacity, the gross potential, is the total reservoir of the buffering compounds in the soil. The unit for the buffer capacity is the same as that for the amount of acid stress (kmol ha^{-1}).

Buffer rate, the rate variable, is defined as the maximum potential rate of the reaction between the buffering compounds and the hydrogen ions. This variable is needed because the reaction kinetics is sometimes of importance. The buffer capacity may be high but the rate may limit the hydrogen ion consumption. Buffer rate is expressed in units which are comparable to those of the stress rate (kmol ha^{-1} $year^{-1}$).

The proton consumption reactions in soils have been systematically described by Ulrich (1981, 1983b). A consecutive series of chemical reactions has been documented for soils subject to acidification. Information regarding the dominant reactions has been used for defining categories, called *buffer ranges*. They are briefly described in the following paragraphs and summarized in Table 1. The name of each buffer range refers to the dominant buffer reaction and the typical pH ranges given refer to the pH of a soil/water suspension ($pH(H_2O)$).

Carbonate buffer range. Soils containing $CaCO_3$ in their fine earth fraction (calcareous soils) are classified into the carbonate buffer range ($pH \geqslant 6.2$). Ca^{2+} is the dominant cation in the soil solution and on the exchange surfaces of the soil particles. The buffer capacity of soils in this range is proportional to the amount of $CaCO_3$ in the soil. In a case where $CaCO_3$ is evenly distributed in the soil, the buffer rate, i.e. the dissolution rate of $CaCO_3$, is high enough to buffer any occurring rate of acid stress.

Silicate buffer range. If there is no $CaCO_3$ in the fine earth fraction and carbonic acid is the only acid being produced in the soil, the soil is classified

TABLE 1

Classification of the acid buffering reactions in forest soils (Ulrich, 1981, 1983b)

Buffer range	pH range	Base saturation	Buffer reaction
Carbonate	8.0–6.2	1.00	$CaCO_3 + H_2CO_3 \rightarrow Ca^{2+} + 2HCO_3^-$
Silicate	6.2–5.0	1.00–0.70	$CaAl_2Si_2O_8 + 2H_2CO_3 + H_2O \rightarrow Ca^{2+} + 2HCO_3^- + Al_2Si_2O_5(OH)_4$
Cation exchange	5.0–4.2	0.70–0.05	clay mineral $= Ca + 2H^+ \rightarrow$ H-clay mineral-$H + Ca^{2+}$
Aluminium	4.2–3.0	0.05–0.00	$AlOOH + 3H^+ \rightarrow Al^{3+} + 2H_2O$
Iron	< 3.8	0.00	$FeOOH + 3H^+ \rightarrow Fe^{3+} + 2H_2O$

into the silicate buffer range ($6.2 > pH \geqslant 5.0$). In this range the only buffer process acting in the soils is the weathering of silicates and the associated release of base cations, since the dissolution of aluminous compounds is not significant until a pH of less than 5.0 is reached. The buffer rate is often quite low, but the buffer capacity is high, as it is formed by the massive storage of the silicate material. The weathering of silicates occurs throughout all buffer ranges. The switch to lower buffer ranges implies that the weathering rate of silicates is not sufficient to buffer the acid stress completely.

Cation exchange buffer range. The soils are classified into the cation exchange buffer range when the cation exchange reactions play the major role in acid buffering: the silicate buffer range is inadequate to buffer the acid stress completely. The excess stress, not buffered by the reactions of the silicate buffer range, is adsorbed in the form of H^+- or Al-ions at the exchange sites, thus displacing the base cations. The cation exchange reactions are fast and, therefore, the buffer rate of soils in this range effectively counteracts any occurring rates of acid stress. The total buffer capacity (= cation exchange capacity, CEC_{tot}) is generally rather low, depending mainly on the soil texture. The remaining buffer capacity at any given time is quantified by *base saturation*, the percentage of base cations of the total CEC. As long as the base saturation stays above 5–10%, the excess stress is buffered by the cation exchange reactions and the soil pH takes a value between 5.0 and 4.2, the actual value depending on the base saturation.

Aluminium buffer range. Below the critical value of base saturation the soils are classified into the aluminium buffer range. Hydrogen ions are consumed

when releasing aluminium mainly from clay minerals. These reactions merely change the form of acidity from hydrogen ions to Al^{3+}. The leachate is thus capable of acidifying adjacent ecosystems. High aluminium ion concentrations characterize the soil solution and may cause toxic effects on bacteria and plant roots. The soil pH is within the range 4.2–3.0.

Aluminium compounds are abundant in soils, so that the buffer capacity rarely restricts the reaction. Buffer rate is decisive: soils do not fall below the aluminium buffer range until the stress rate exceeds the production rate of highly dissolvable Al-hydroxy-compounds.

Iron buffer range. At the extreme stage of acidification, soils may be classified into the iron buffer range. Increasing solubility of iron oxides is observed. This leads to visible (colour) symptoms in the soil profile, which is not the case for aluminium, although in quantitative terms aluminium may still act as the dominant buffer compound. The pH-values as low as 3.0 indicate that living organisms will suffer from toxicity and nutrient deficiency.

MODEL DEVELOPMENT

Basic assumptions

The requirement of a large spatial scale necessitates several simplifications in the model. The assumptions affecting the model structure itself are briefly described here, whereas the additional assumptions included in the model application at its present stage are discussed in a subsequent chapter.

The soil is considered as a homogeneous box. It is, however, possible to divide the soil into several layers if it is considered important when estimating the effects of soil acidification. In fact, this has already been done in connection with the RAINS surface water acidification model (Kämäri et al., 1985), where two layers were introduced.

The ion exchange and buffering properties of organic matter are not taken into account separately from the inorganic buffer systems. Information on the humus content of the soil or the thickness of the moor layer is not commonly available from different parts of Europe. At least in northern Europe, where the accumulation of organic matter is significant, it would be important to take the buffering properties of organic matter into account.

The model was designed to focus on the year-to-year changes in soil acidity. Seasonal, monthly or even daily patterns of soil acidity are potentially very important as they may effectively act as key situations triggering biological effects. Our model describes the annual baseline level for the short-term peaks of low or high acidity. In this way it does not directly focus

on the potentially crucial events but it estimates trends of increasing probabilities of such events. This restriction of focus made it possible to exclude redox processes and sulphate adsorption processes from the model. It was assumed that these processes generate seasonal variability in soil acidity which levels out in the long run without affecting the year-to-year trend.

The weathering rate of silicates and the connected release of base cations is assumed to be independent of the soil pH. In some laboratory experiments it has been shown that the release of silicates increases with decreasing pH (e.g. Wollast, 1967; Busenberg and Clemency, 1975; Stumm et al., 1983). However, the release of silica does not necessarily imply that base cations are released at the same rate. They may precipitate with aluminium compounds to form clay minerals. Increased base cation leaching is usually due to cation exchange reactions, not necessarily to increased weathering rate. In Solling, Federal Republic of Germany, no deviation in the weathering rate of silicate from the long-term average has been observed, although the pH of the soil has decreased (Matzner, unpublished).

MODEL STRUCTURE

The model describes soil acidification in terms of the sequence of the buffer ranges. It compares (a) the amount of stress (cumulative value over the time period of interest) with the buffer capacity, and (b) the stress rate (year-to-year basis) with the buffer rate. The comparisons are made separately for the carbonate, silicate and cation exchange buffer ranges. The model thus assumes that values for the buffering variables – buffer capacity and buffer rate – are determined separately for each of these buffer ranges. For the aluminium and iron ranges, and equilibrium approach was chosen. The soil pH is assumed to stay in equilibrium with solid phases of aluminium compounds.

All the buffering variables do not have to be considered in the model. The buffer rates of the carbonate range and the cation exchange range are so high that in practice they cannot be exceeded by any occurring rate of acid stress. Moreover, the buffer capacities of silicate and aluminium ranges cannot be exhausted in the time scale of hundreds of years. The iron range is assumed to be quantitatively irrelevant for buffering at pH-values above 3.0. In this way the number of buffering variables actually included into the model reduces to four. The excluded variables receive values high enough not to affect the model output.

The model is used by taking the given pattern of acid stress as the input variable. The program compares the (annual) acid stress with the buffer rate determined for the prevailing buffer range. It also compares the accumulated

amount of acid stress with the buffer capacity. With these comparisons the program calculates which buffer range prevails each year, and then computes the approximation of the prevailing soil pH.

Acid stress to the top soil is partly or totally neutralized by the weathering of carbonate or silicate minerals. It is assumed that soils containing free carbonates (calcareous soils) always have a buffer rate high enough to neutralize any rate of acid stress; in this case the soil pH is assumed to stay at 6.2 as long as the buffer capacity of this range is not exhausted. In

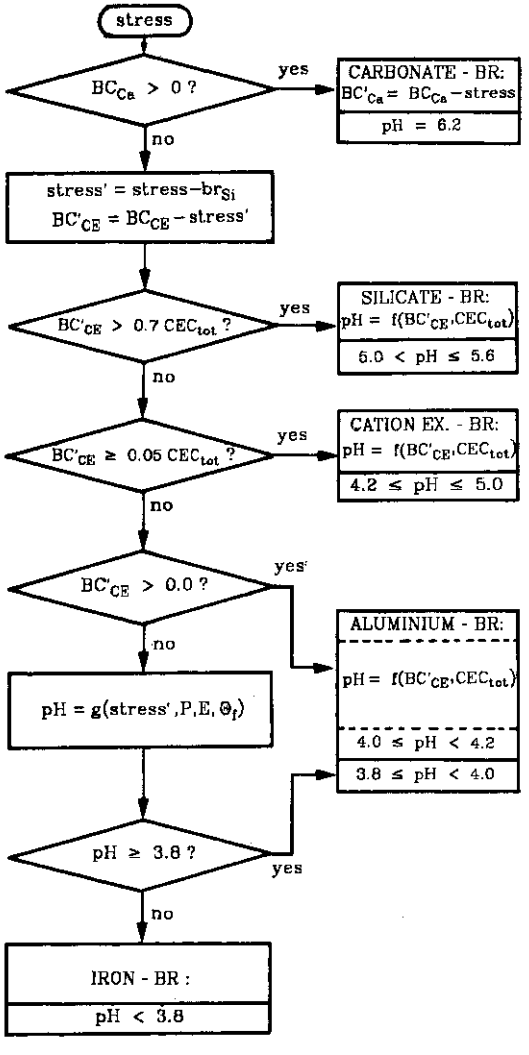

Fig. 1. Flow diagram of the soil acidification model.

non-calcareous soils, neutralization depends on the intensity of silicate weathering (silicate buffer rate). As long as this buffer rate is greater than the acid stress no decrease in soil pH is assumed to occur.

If the acid stress exceeds the actual buffer rate of silicates, the hydrogen ions gradually replace the base cations of the exchange sites of the soil particles thus decreasing the base saturation of the soil. The capacity of the cation exchange buffer system is depleted at a rate equal to the difference between the acid stress rate and the buffer rate of silicates. Buffering within the silicate buffer range, essentially due to weathering of the silicate mineral, acts through all the buffer ranges. In other words, the cation exchange capacity is a result of an input of cations from chemical weathering as well as of a depletion of cations by ion exchange. The same gradual character was introduced for the recovery. The soil pH is then estimated on the basis of the prevailing base saturation within the cation exchange range and the upper aluminium range at pH 5.6–4.0. If the cation exchange capacity is totally exhausted the hydrogen ion concentration is assumed to be determined by equilibrium with solid phase aluminium which implies dissolution or precipitation of aluminium until an equilibrium state is reached. The specific equations incorporated into this model structure are presented as an Appendix. The main characteristics of the model are summarized in the flow chart (Fig. 1).

MODEL DEMONSTRATION

The dynamic features of the model are demonstrated in this section by producing two input–output patterns. These figures describe the reactions of only one soil type, Dystric Cambisol (Bd). Table 2 indicates the characteristics of this soil type assumed to prevail at the beginning of the 100-year

TABLE 2

Initial conditions and parameter values for model demonstration (Soil type: Dystric Cambisol, Bd)

Carbonate buffer capacity	BC_{Ca}	0.0	kmol ha^{-1}
Silicate buffer rate	br_{Si}	1.0	kmol ha^{-1} $year^{-1}$
Cation exchange buffer capacity	BC_{CE}	170.0	kmol ha^{-1}
Total cation exchange capacity	CEC_{tot}	1100.0	kmol ha^{-1}
Volumetric water content at field capacity	Θ_f	0.27	
Precipitation; Central Europe	P	0.90	m $year^{-1}$
Evapotranspiration; Central Europe	E	0.50	m $year^{-1}$

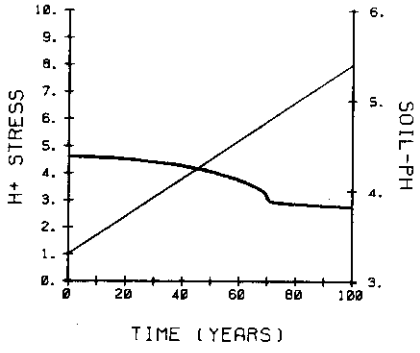

Fig. 2. Input–output relationship: response of the soil to an increasing stress (thick line = soil pH).

study period. When fixing these values the thickness of the reacting soil layer was assumed to be 50 cm. BC_{Ca} being zero indicates that Dystric Cambisol is free of lime. The input for this model demonstration consists of two hypothetical time patterns of the acid stress for the period of 100 years. The output is the time pattern of the soil pH, corresponding to the mean hydrogen ion concentration in the 50-cm soil layer.

Figure 2 indicates that for this soil the pH gradually declines from 4.6 to 4.0 in 100 years while the soil is subject to a growing stress from 1 to 8 kmol ha^{-1} $year^{-1}$. The silicate buffer range accounts for the buffering of 1 kmol ha^{-1} $year^{-1}$ of the acid stress. The excess stress is buffered by the processes of the cation exchange range. After 60 years the buffer capacity of the cation exchange range is decreased to a base saturation level of 5%. At this point, none of the higher buffer ranges is capable of buffering the stress, and the soil pH declines to the level which corresponds to the pH range of the aluminium buffer system. The acid stress, partly buffered within the silicate buffer range, finally determines a new equilibrium pH in the soil solution according to the aluminium solubility assumed. This process results in a slowly decreasing soil pH due to the growing stress rate.

A dramatic pattern of acid stress was selected to summarize the dynamic behaviour of the model (Fig. 3). The pattern includes a constant stress of 8 kmol ha^{-1} $year^{-1}$ for 30 years, a linear decline to zero in the subsequent 40 years, and a constant zero stress over the remaining 30 years. The soil with initial conditions as in Table 2 reacts in the following way: First, there is a gradual but accelerating decline in pH from 4.6 to 4.2, and then there is a rapid decline of pH to the aluminium buffer range, near to pH 3.7. The buffer capacity of the cation exchange range is exhausted and the buffer rate of the aluminium range cannot keep the pace with the acid stress rate. Next, there is an increase of the soil pH to 4.0. By that time the acid stress has

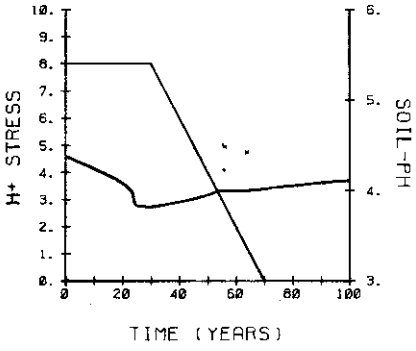

Fig. 3. Input–output relationship: response of the soil to a declining stress (thick line = soil pH).

declined so that the joint buffering of the silicate and the aluminium ranges is capable of increasing the pH. Finally, a recovery starts from pH 4.0 upwards. This is possible because the acid stress declines to the level where the silicate buffer rate alone is capable of buffering the stress. During the gradual recovery in the soil, weathering slowly replaces hydrogen ions by base cations on the exchange sites. The cation exchange capacity is refilled, starting at pH 4.0, at a rate equal to the difference between the buffer rate of the silicate range and the rate of the acid stress. A base saturation level of 4% will be reached by the end of the 100-year period.

MODEL APPLICATION

This application is part of the Regional Acidification INformation and Simulation (RAINS) model system of the IIASA Acid Rain Project which has the general objective of analyzing alternative control strategies of the European sulfur emissions. The focus of the application is hence restricted to the stress due to air pollution. The IIASA framework sets the prerequisite of a large spatial scale. The project has provided an energy-emission model for generating scenarios of future sulfur emissions in Europe assuming optional programs for energy development and sulfur control (Alcamo et al., 1985). The computed emissions are converted to sulfur deposition scenarios by using the long-range transport model for air pollutants developed within the EMEP-program (see Eliassen and Saltbones, 1983). This model has been applied to RAINS by reducing it to a source receptor matrix (Alcamo et al., 1985). Sulfur deposition is then transformed into an approximation of the acid stress, and this information is used as the driving variable of the soil acidification model (Fig. 4).

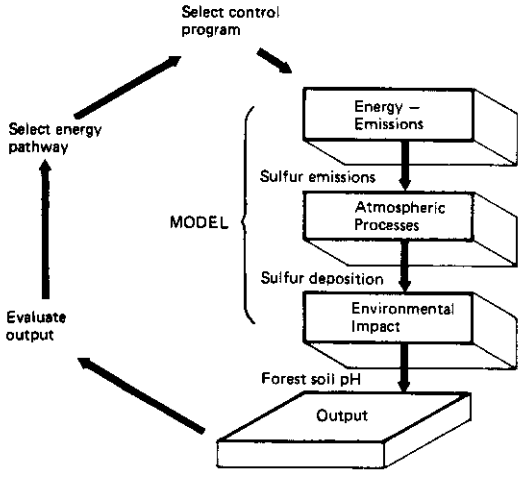

Fig. 4. The IIASA acid rain framework and procedure for using the model.

Specific assumptions

For the time being, the acid stress was estimated on the basis of sulfur deposition only, simply by assuming acid stress to be proportional to sulfate ion equivalents in the water entering the soil. The actual acid stress associated with sulfur deposition depends on the neutralization intensity of e.g. atmospheric dust and canopy. The spatial variation of these processes was not taken into account. A single relationship was assumed, as the first step for the whole of Europe. This acid stress coefficient, σ, seems to have values between 0.5 and 0.75 in some European forests (Wright and Johannessen, 1980). Internal proton production, i.e. proton production resulting from the excess accumulation of cations in the biomass and humus, was not included in the estimates of acid stress.

The EMEP model assumes constant deposition velocity over all land surfaces (Eliassen and Saltbones, 1983). This assumption is necessary as the model covers the whole of Europe; it would be an enormous task to describe the spatial variability of the deposition velocity in detail. Model validation suggests that, in general, the assumption of constant deposition velocity can be supported when aiming at modelling the concentrations of sulfur compounds on a large spatial scale. From local experiments, however, it appears that forests have a rather strong filtering effect on air pollutants, so that the deposition velocity over forests is larger than that of open land by a factor of two to three, depending on the tree species. As forests were the main target ecosystem for our model, we considered it necessary to include the filtering effect in the model.

Based on the validation experiments of the EMEP model the average total deposition of a grid square, d_{tot}, was assumed correct. The deposition on the forest within this grid, d_f, was then assumed to be ϕ times larger than the deposition on open land, d_o (1)

$$d_f = \phi d_o \tag{1}$$

Since

$$fd_f + (1-f)d_0 = d_{tot} \tag{2}$$

where f is the fraction of forest within the grid, we get for d_f

$$d_f = d_{tot}\phi/(1 + (\phi - 1)f) \tag{3}$$

from which acid stress, s, was derived by assuming that a fraction σ of the acidifying sulfur deposition enters the soil unneutralized.

$$s = \sigma d_f \tag{4}$$

The above calculation procedure takes into account (a) the estimated gross deposition on each grid square, (b) the filtering factor ϕ, (c) the fraction of forests in each grid square, f, digitalized from the World Forestry Atlas (1975), and (d) the acid stress factor, σ. It produces as an output the allocation of deposition between forests and agricultural land within each grid square. This specific feature of the IIASA model gives the first priority to the long-range transport model as far as large-scale variability of deposition is concerned and yet describes the filtering effect of forests by including small scale information on the distribution of forests vs. open land within the grid square. A factor $\phi = 2$ is used as long as detailed information on the spatial distribution of ϕ is not available. For the acid stress coefficient, σ, a value of $\sigma = 2/3$ was chosen as a tentative approximation.

It is conceivable that forests, as they represent areas neglected by agriculture, grow on particularly susceptible soils. Soils which have low specific weathering rates and low levels of base saturation are more susceptible to acidification than are soils otherwise. The concentration of forests on poor soils, although hypothetical, was considered so obvious that it was included as part of the model. Rather than assuming the fraction of forests constant on all soil types we used the following calculation procedure: forests of a given grid square were allocated starting from soil types with the lowest weathering rates and cation exchange capacity values and continuing until all forests were distributed. In this way agriculture was located on the most fertile soils while poor soils of a grid were assumed for forests.

In the presentation of results an important indicator is the 'critical acidity'. At present the switch to the aluminium buffer range (base saturation 0.05, pH 4.2) is assumed to imply an increased risk of forest damage.

There are several reasons why this degree of acidity was assumed to be critical: soil chemistry changes quite drastically; Al-concentration in the soil solution increases and Ca/Al-ratio reaches the level that implies the risk of soil-borne toxicity to tree roots (Ulrich et al. 1984; Matzner and Ulrich, 1985). More research, however, would be needed to relate the risk of forest damage to the soil acidity. The final decision about the 'critical pH' is left to the model user.

Initialization of buffering variables

Initialization of the soil variables was based on the chemistry information available on European soils, and on the soil thickness selected to approximate the rooting zone. The buffer capacity of the carbonate range is proportional to the lime content of the soil; the buffer rate of the silicate range is related to the chemical weathering rate of the silicate minerals; the buffer capacity of the cation exchange rate depends on the clay content and base saturation of the soil; and the buffer rate of the aluminium range depends on the accessibility of aluminium compounds. Although such relationships, especially those regarding the aluminium accessibility are only partially understood, they can be used as a guideline in quantifying the susceptibility of the soils to acidification. The values for the buffer capacities and buffer rates were initialized accordingly based on the International Geological Map of Europe and the Mediterranean Region (1972) and the FAO-Unesco Soil Map of the World (1974). The depth of the reacting soil was assumed to be 50 cm throughout the study area. The year 1960 was selected as the baseline year.

Detailed soil chemistry information regarding the other soil variables was available from the Soil Map. The fraction of each soil type within the grid square was computerized with an accuracy of 5%. The resolution of the map is such that a standard grid square was composed of 1–7 soil types. The number of different soil types was 80. The soil data base consists of 5212 soil units, the mean number of soil types per grid square being 2.2. One 70-year simulation for the whole of Europe thus requires about 365 000 model runs.

All information regarding soils was stored in a computerized grid-based format. Each grid square had the extension of 1° longitude times 0.5° latitude. In this way the size of a grid was fixed at 56 km in the south-north direction, but in the east-west direction it varied from 91 to 38 km depending on the latitude. The number of grid squares was 2304.

Initial values for the soil variables were given for every soil type (Table 3). The Soil Map, however, could not provide the information regarding the buffer rate of the silicate buffer range which is equal to the weathering rate

TABLE 3

Buffer capacities of the carbonate and the cation exchange buffer ranges estimated for the year 1960 for soil types of the FAO-Unesco Soil Map of the World (1974). Soil thickness of 50 cm is assumed.

Soil type	BC_{Ca} (kmol ha^{-1})	BC_{CE}	Soil type	BC_{Ca} (kmol ha^{-1})	BC_{CE}	Soil type	BC_{Ca} (kmol ha^{-1})	BC_{CE}
Ao	200.0	910.0	Kk	8000.0	1170.0	Vc	32000.0	1170.0
Bc	500.0	1225.0	Lc	3000.0	170.7	Vp	9000.0	3640.0
Bd	0	165.8	Lf	0	138.8	Wd	0	47.3
Be	500.0	1824.0	Lg	0	146.3	We	500.0	1410.5
Bg	500.0	180.0	Lo	0	107.3	Xk	43000.0	1170.0
Bh	0	136.5	Lv	3000.0	1225.0	Xy	40000.0	1225.0
Bk	25000.0	1470.0	Mo	0	1495.0	Zg	15000.0	1225.0
Bv	0	2210.0	Od	0	72.0	Bc-Lc	3000.0	685.6
Ch	0	390.0	Oe	0	168.8	I-Bc	200.0	1050.0
Ck	19000.0	2535.0	Pg	0	180.0	I-Bc-Lc	1500.0	469.1
Cl	0	419.3	Ph	0	49.0	I-Bd	0	151.2
Dd	0	136.5	P	0	68.3	I-Be	0	765.6
De	0	136.5	Po	0	78.0	I-Be-Lc	1500.0	533.9
Dg	0	468.0	Pp	0	239.2	I-Bh-U	0	136.5
E	20000.0	2600.0	Qc	100.0	227.5	I-C	500.0	910.0
Gd	0	126.8	Ql	0	117.0	I-E	10000.0	1750.0
Ge	0	302.3	Rca	0	47.3	I-L	0	149.3
Gh	0	146.3	Rcb	0	136.5	I-Lc	1500.0	153.6
Gm	0	183.8	Rcc	500.0	857.5	I-Lo-Bc	0	408.5
Hc	7000.0	1170.0	Re	0	136.5	I-Lc-E	10000.0	1500.0
Hg	500.0	1820.0	So	500.0	1183.0	I-Po	0	126.8
Hh	1000.0	321.8	Sm	0	236.3	I-Po-Od	0	108.5
Hl	0	312.0	Th	0	127.5	I-Rc-Xk	20000.0	1500.0
I	0	136.5	Tm	0	136.5	I-Re-Rx	0	106.8
Jc	8000.0	315.0	To	0	183.8	I-U	0	136.5
Je	200.0	1008.0	Tv	0	120.0	Lo-Lc	1500.0	139.1
Kh	0	136.5	U	0	136.5			

of the parent material. The approximation of this variable was based on other sources. Ulrich (1983b) reports a range of variation in European soils from 0.2 to 2.0 kmol ha^{-1} $year^{-1}$ m^{-1}. Four classes for the reacting 50-cm soil layer were introduced with the following buffer rates (in kmol ha^{-1} $year^{-1}$):

class	1	2	3	4
buffer rate	0.25	0.50	0.75	1.00

The Geological Map was used to determine parent materials of soils in each grid square. Depending on the dominant parent material the soil of each grid square was classified into one of the above categories.

Based on this information the model is applicable for producing acidification scenarios for forest soils. The model is run separately for each soil type within the grid square. An estimate of soil pH is the output.

Results of model runs

Two example scenarios were introduced using the IIASA energy-emission model, and the long-range transport model supplied by the EMEP program. From 1960 until 1980 the scenarios were identical. From then on the scenarios diverged so that the 'high' deposition scenario assumed high rates of energy development throughout Europe, as defined by the ECE 'trends continued' scenario (ECE, 1983) linearly extrapolated to 2030. The 'low' deposition scenario was constructed according to the ECE 'conservation' scenario, assuming lower rates of energy use and, in addition to that, effective measures taken for the control of sulfur emissions (Fig. 5). The specific method of generating different scenarios is presented elsewhere (Alcamo et al., 1985).

The model can be used for producing an estimate of the pH ranges of forest soils in Europe for any selected scenario and year (Fig. 6). An

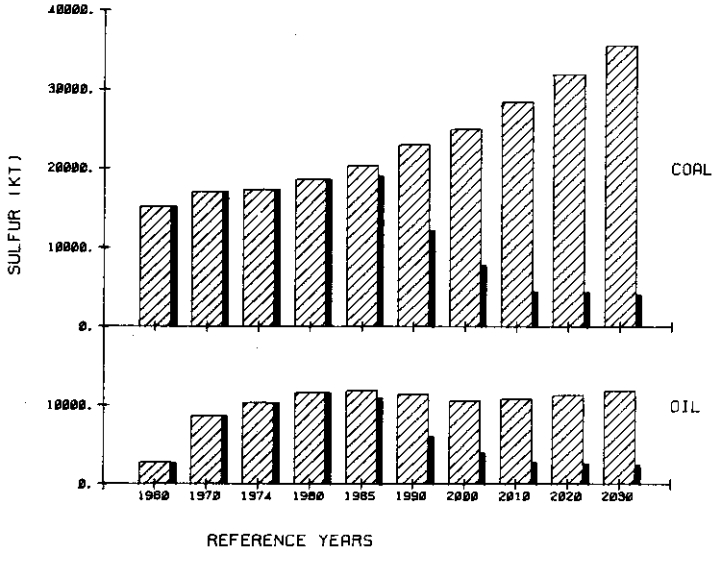

Fig. 5. Total sulfur emitted in Europe according to the 'high' and 'low' emission scenario from coal and oil sectors.

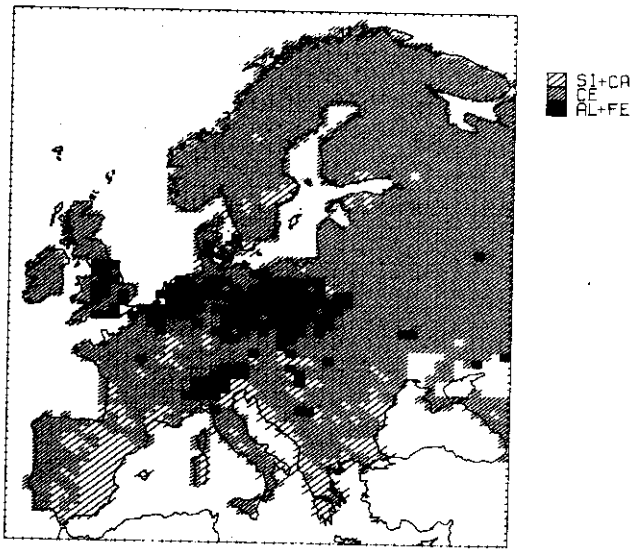

Fig. 6. Model estimates of the soil acidity in Europe in 1980. Si + Ca represent the silicate and carbonate buffer ranges, CE cation exchange buffer range, and Al + Fe aluminium and iron buffer ranges.

additional option is to display the areas with soils in a critical buffer range or areas with soils below a critical pH. This concept bears on the notion that the risk of forest damage increases below a critical acidity. A default value of 4.2 is introduced for the critical pH but the model user can interactively select other values. The area below a critical pH value can be displayed in map format, with different shadings indicating the percentage of the total forest area with soil pH below the selected value (Fig. 7).

For summarizing the results an option has been added to display estimates of the time patterns of the total forest area with soils below the critical acidity (Fig. 8). The area of the forest in each grid square is calculated and the time evolution of the area of European forests with soil pH below a selected critical value is then displayed.

As part of the IIASA study this application of the soil acidification model is designed for quick comparisons of sulfur emission scenarios. It is up to the model user to decide what kind of scenarios should be compared. The two examples were selected to demonstrate the model behaviour. Therefore, the examples are relatively useless as far as selection of feasible policy options is concerned. In the following paragraphs we will discuss the effects of the 'low' vs. the 'high' scenario but this discussion is intended merely to demonstrate the properties of the model.

By the year 1980, that is assuming the historical deposition pattern, the model predicts a decline in the soil pH over relatively large regions of

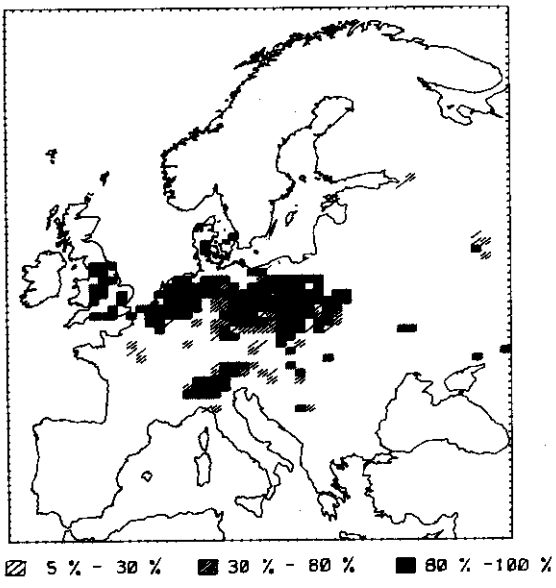

Fig. 7. Model estimates of forest soils below pH 4.2 in 1980. The shading determines the fraction of forest soils below the threshold pH in each grid.

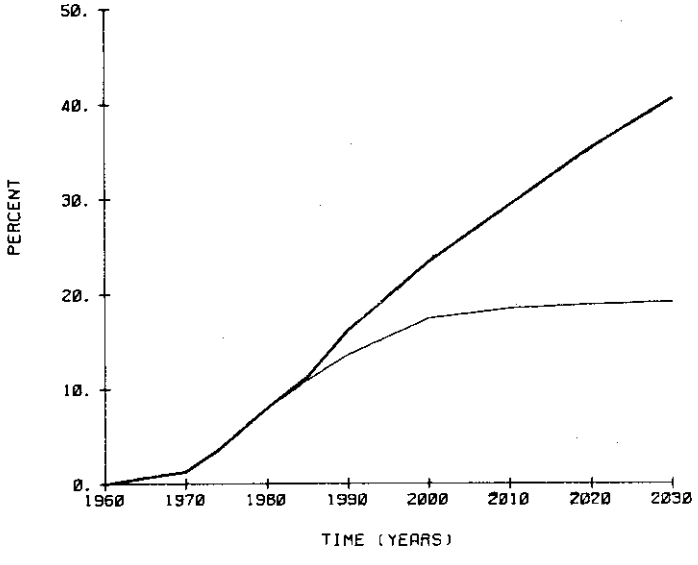

Fig. 8. Time evolution of the total forest area with soils in aluminium and iron buffer range (pH less than 4.2) in Europe assuming the two emission scenarios.

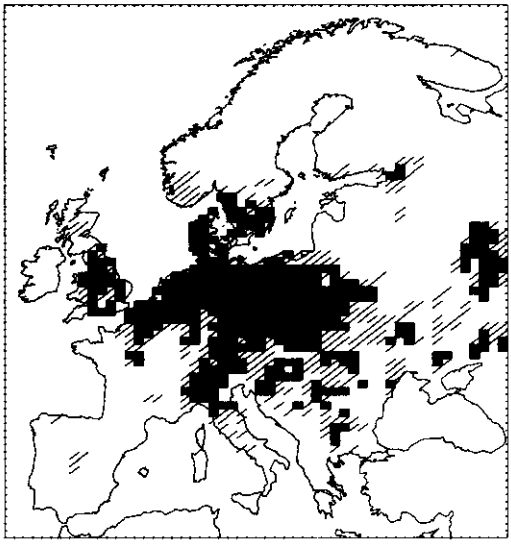

Fig. 9. A comparison of the area at risk in 2010, aluminium and iron being the dominant buffer ranges, resulting from the high emission scenario (light shading) and from the low emission scenario (dark shading).

Central Europe. Continuing with the 'high' deposition scenario the area of low pH substantially enlarges by the year 2010 and much of the soils in Central Europe and Southern Scandinavia reach the aluminium buffer range (Fig. 9).

The region where the soils fall into the aluminium buffer range (pH below 4.2) already appears on the map by 1970. This area, interpreted as the area at risk of forest damage, increases by 1980 (Fig. 7) and, with the 'high' deposition scenario, it is enlarged substantially by the year 2010 (Fig. 9). An option has been added in the computer program for direct comparison of the estimated areas at risk from two scenarios. When the 'low' scenario is used as the input, the results indicate much less risk of forest damage by the year 2010 (Fig. 9). As indicated by Fig. 8 the forest area with soils more acidic than the threshold is estimated to be twice as large with the 'high' scenario as with the 'low' scenario.

DISCUSSION

The model developed in this study can be used for quantifying some aspects of the acidification problem of forest soils previously discussed in only qualitative terms. The soil acidification model and the application to the European overview are simplifications, which necessarily include uncer-

tainties. Many solutions, as they stand now, are crude approximations which need clarification in future research. It is the hope of the authors, however, that the model structure would act as a tool for organizing the data and for identifying research needs. Even in its present stage the model might appear useful in evaluating policies to combat the acidification of forest soils.

The model makes a distinction between reversible and irreversible changes in the soil chemistry. Exhaustion of the buffer capacity is in some cases irreversible. The case of an insufficient buffer rate, in turn, may be reversible: the buffer rate is again sufficient when the stress rate (annual load) is reduced below a threshold which is the value of the buffer rate variable. This feature of the model should be useful as it indicates whether a decrease in the acid stress would result in a recovery of the soil, or whether it would merely cause a delay in the acidification process.

The model, designed for forest soils, appears too complex for agricultural soils. Intensive agriculture maintains high pH values in soils by means of liming and other practices. In theory, the model could be used for calculating, for example, the amount of lime needed to counteract the acidic deposition. This calculation, however, can be done using more straightforward methods.

The application of the model to the problem of acidic deposition in Europe indicates that soil buffering fails to maintain adequate pH levels in large parts of Central Europe. In northern Europe, although the buffering is generally less efficient, the acidic deposition would cause less trouble in this respect. This does not prove that the problem of soil acidification is restricted to Central Europe. Acidification due to biomass accumulation, i.e. the so-called internal proton production, has a special role in northern Europe where low temperatures retard biomass decomposition. High internal proton production increases the susceptibility of the environment to the acidification due to air pollutants. This additional stress needs to be addressed in future research.

The soil variables were initialized for 1960. This does not imply that no acid stress was assumed before that time. The initialization should be viewed as fixing a reference point rather than a manifestation of the state of virgin forests. The initialization should be based on field measurements; in the present application this goal was only partially fulfilled.

The reacting volume was fixed at the top 50 cm of the soil. No horizontal gradients were explicitly assumed. Increasing the reacting volume would postpone the possible problem. Including the gradients would involve faster acidification in the very top of the soil and slower acidification in the deeper layers. The above results correspond to the average situation in the volume. This average value may be inaccurate in some cases due to the nonlinearities of the model.

The model lacks hydrologic considerations since it is only dealing with the uppermost soil layer. However, soil permeability and watershed slope may be important factors in determining the leaching rates of base cations from the soil horizon. Moreover, the model assumes that all deposition actually reacts within the top soil. This may not always be the case. The higher the rate of water input and the coarser the soil texture, the less favourable are the conditions to reach chemical equilibrium between the solutes and the soil matrix. If part of the deposition flows unchanged through the top soil, the soil response will be delayed and the acidification problem is transferred into the adjacent ecosystems or to the groundwater. An effort is currently under way within the IIASA Acid Rain Project to apply the soil acidity model as a component of a regional model of surface water acidification.

Soil acidification poses a threat to forest ecosystems and generates predisposing stress in ecosystems as defined by Manion (1981). Forest damage, however, is a multicausal phenomenon. Many factors are involved such as ozone pollution, heavy metals, exceptional climatic conditions, and cultivation of tree species outside their natural habitats. The interactions of soil acidification and the other factors deserve concerted research effort. It does not seem possible today to describe the forest damage in satisfactory detail with any specific model. But emphasizing the complexity of the forest damage as an argument against serious modelling efforts may well cause a delay in obtaining a better understanding of the phenomenon.

ACKNOWLEDGEMENTS

Professor B. Ulrich from the University of Göttingen encouraged the development of this study, and contributed significantly to the successful collaboration between IIASA and the University of Göttingen. We gratefully acknowledge his support.

We would also like to thank Dr. N. van Breemen and Dr. I. Nilsson for their valuable advice during the development of this study.

REFERENCES

Alcamo, J., Hordijk, L., Kämäri, J., Kauppi, P., Posch, M. and Runca, E., 1985. Integrated analysis of acidification in Europe. J. Environ. Manage., 21: 47–61.

Busenberg, E. and Clemency, C.V., 1975. The dissolution kinetics of feldspars at 25°C and atmospheric CO_2 partial pressure. Geochim. Cosmochim. Acta, 40: 41–49.

ECE, 1983. An Efficient Energy Future. Butterworths, London, 259 pp.

Eliassen, A. and Saltbones, J., 1983. Modeling of long-range transport of sulphur over Europe, a two year model run and some model experiments. Atm. Environ., 17: 1457–1473.

Kämäri, J., Posch, M. and Kauppi, L., 1985. Development of a model analyzing surface water acidification on a regional scale: application to individual basins in Southern Finland. In: Proc. Workshop 15–16 September, 1984, Uppsala. NHP Report 10, Nordic Hydrological Programme, Copenhagen, pp. 151–170.

Lammel, R., 1984. Endgültige Ergebnisse und bundesweite Kartierung der Waldschadenserhebung, Allg. Forst Z., 39: 340–344.

Manion, P.D., 1981. Tree Disease Concepts, Prentice-Hall, London, 368 pp.

Matzner, E., 1983. Balances of element fluxes within different ecosystems impacted by acid rain. In: B. Ulrich and J. Pankrath (Editors), Effects of Accumulation of Air Pollutants in Forest Ecosystems. Proc. Workshop, 16–19 May 1982, Göttingen. Reidel, Dordrecht, The Netherlands, pp. 147–155.

Matzner, E. and Ulrich B., 1984. Implications of the chemical soil condition for forest decline. Experimentia (submitted).

OECD, 1979. The OECD programme on long range transport of air pollutants. Measurements and findings. Paris, 164 pp.

Reuss, J.O., 1983. Implications of the calcium–aluminium exchange system for the effect of acid precipitation on soils. J. Environ. Qual., 12: 591–595.

Schütt, P., 1977. Das Tannensterben, Der Stand unseres Wissen über eine aktuelle und gefährliche Komplex-Krankheit der Weisstanne (*Abies alba*). Forstwiss. Zentralbl., 96: 177–186.

Schütt, P., Blaschke, H., Hoque, E., Koch, W., Lang, K.J. and Schuck, H.J., 1983. Erste Ergebnisse einer botanischen Inventur des 'Fichtensterbens'. Forstwiss. Zentralbl., 102: 201–213.

Stumm, W., Furrer, G. and Kunz B., 1983. The role of surface coordination in precipitation and dissolution of mineral phases. Croat. Chim. Acta 56: 593–611.

Ulrich, B., 1981. Theoretische Betrachtungen des Ionenkreislaufs in Waldökosystemen. Z. Pflanzenernähr. Bodenkd., 144: 647–659.

Ulrich, b., 1983a. A concept of forest ecosystem destabilization and of acid deposition as driving force for destabilization. In: B. Ulrich and J. Pankrath (Editors), Effects of Accumulation of Air Pollutants in Forest Ecosystems. Proc. Workshop. 16–19 May 1982, Göttingen. Reidel, Dordrecht, The Netherlands pp. 1–29.

Ulrich., B. 1983b. Soil acidity and its relation to acid deposition. In: B. Ulrich and J. Pankrath (Editors), Effects of Accumulation of Air Pollutants in Forest Ecosystems. Proc. Workshop, 16–19 May, 1982, Göttingen. Reidel, Dordrecht, The Netherlands pp. 127–146.

Ulrich, B., Miewes, K.J., König, N. and Khanna, P.K., 1984. Untersuchungsverfahren und Kriterien zur Bewertung der Versauerung und ihrer Folgen in Waldböden. Forst Holzwirt, 39: 278–286.

Van Breemen, N., Driscoll, C.T. and Mulder, J., 1984. Acidic deposition and internal proton sources in acidification of soils and waters. Nature (London), 307: 599–604.

Wollast, R., 1967. Kinetics of the alteration of K-Feldspar in buffered solutions at low temperatures. Geochim. Cosmochim. Acta, 31: 635–648.

Wright, R.F. and Johannessen, 1980. Input–output budgets of major ions at gauged catchments in Norway. In: D. Drabløs and A. Tollan (Editors). Ecological Impact of Acid Precipitation. Proc. Conf. Sandefjord, Norway, 11–14 March, 1980. SNSF-project, Oslo-Ås, pp. 250–251.

Maps:
FAO-Unesco, *Soil Map of the World*, Vols. I, V. Paris, 1974.
Bundesanstalt für Bodenforschung Hannover, *International Geological Map of Europe and the Mediterranean Region*. Unesco, Paris, 1972.
Weltforstatlas (*World Forestry Altas*), Paul Parey, Hamburg/Berlin, 1975.

APPENDIX

The capacity of the cation exchange buffer system, BC_{CE}^{t}, is depleted with the rate of acid stress, s^t, minus the buffer rate of silicates, br_{Si} (A1). A non-linear relationship is assumed between the base saturation and the soil pH within the silicate, cation exchange and the upper aluminium buffer range, as long as $BC_{CE}^{t} \geqslant 0$, at pH 5.6–4.0 (A2):

$$BC_{CE}^{t} = BC_{CE}^{t-1} - \left(s^t - br_{Si}\right) \tag{A1}$$

$$pH = 4.0 + 1.6\left(BC_{CE}^{t}/CEC_{tot}\right)^{3/4} \tag{A2}$$

The shape of the pH-base saturation relationship has been adopted from results of an equilibrium model by Reuss (1983).

If $BC_{CE}^{t} = 0$, equilibrium with gibbsite is assumed. As precipitation infiltrates into the soil and mixes with the soil solution, disequilibrium concentrations $[Al^{3+}]_s$ and $[H^+]_s$ are obtained (A3, A4):

$$[Al^{3+}]_s = V_f[Al^{3+}]^{t-1}/(V_f + (P - E)) \tag{A3}$$

$$[H^+]_s = \left(V_f[H^+]^{t-1} + \left(s^t - br_{Si}\right)\right)/(V_f + (P - E)) \tag{A4}$$

where V_f is the volume of soil solution at field capacity and P and E mean annual precipitation and evapotranspiration, respectively. On an annual basis the infiltrating water volume is assumed to equal $P - E$. The soil solution volume is simply defined by:

$$V_f = \Theta_f z \tag{A5}$$

The soil thickness, z, is fixed at 50 cm and the volumetric water content value at field capacity, Θ_f is estimated separately for each soil type based on the grain size distribution of the soil. Aluminium is dissolved or precipitated until the gibbsite equilibrium state (A6) is reached.

This process involves a change from disequilibrium concentrations as defined in equation (A7):

$$[Al^{3+}]'/([H^+]')^3 = K_{so}, \quad K_{so} = 10^{+8.5} \tag{A6}$$

$$3([Al^{3+}]_s - [Al^{3+}]') = [H^+]' - [H^+]_s \tag{A7}$$

Combining equations (A6) and (A7) yields a third-order equation which has a single real root (A8):

$$3K_{so}([H^+]')^3 + [H^+]' - 3[Al^{3+}]_s - [H^+]_s = 0 \tag{A8}$$